Journal of Coastal Research	SI	95	1240–1244	Coconut Creek, Florida	2020

Modelling Storm Waves in the Nearshore Area Using Spectral Models

Marc Pezerat[†*], Kévin Martins[†‡], and Xavier Bertin[†]

[†]UMR 7266 LIENSs
CNRS – La Rochelle Université
France

[‡]UMR 5805 EPOC
CNRS – Université de Bordeaux
France

www.cerf-jcr.org

www.JCRonline.org

ABSTRACT

Pezerat, M.; Martins, K., and Bertin, X., 2020. Modelling storm waves in the nearshore area using spectral models. *In:* Malvárez, G. and Navas, F. (eds.), *Global Coastal Issues of 2020. Journal of Coastal Research,* Special Issue No. 95, pp. 1240-1244. Coconut Creek (Florida), ISSN 0749-0208.

This paper presents field observations collected in 2010 in the shoreface of Oléron Island (France) under storm wave conditions combined with predictions from the state-of-the-art spectral model WWM-III to evaluate three classical formulations for dissipation by depth-induced breaking. This comparison reveals a substantial over-dissipation by breaking resulting in a negative bias on significant wave height reaching 50% at the peak of the storm. An adaptive parameterization based on existing theories for depth-induced breaking has consequently been tested and yields improved predictions. This new parameterization remains to be tested under various incident wave conditions up to the inner surf zone.

ADDITIONAL INDEX WORDS: *Depth-induced breaking, storm waves, spectral modelling.*

INTRODUCTION

Short waves play a fundamental role in the nearshore dynamics particularly under storm conditions where they contribute to extreme water levels (Bertin *et al*., 2015) and drive large morphological changes (Masselink *et al*., 2016). As human activities are inexorably broadening in the nearshore area, it is essential to model accurately the propagation and dissipation of short waves in this area, in particular during storms. However, the accuracy of numerical models to simulate storm waves-induced hydrodynamics in those areas remains uncertain, which is partly explained by the scarcity of field observations. For regional to local scale studies, the computation of wave fields using spectral model flourished thanks to the theoretical and numerical advances on wave-current interaction and on the use of unstructured meshes to discretize the geographical space (*e.g.* Roland and Ardhuin, 2014). Such models allow to represent the sea state by means of the action spectrum. The Wave Action Equation gives the evolution in space and time of the action spectral densities. In particular, the evolution of action spectrum is modified by source terms accounting for wave growth and dissipation processes. Close to sandy shores, incident waves dissipate their energy mostly through depth-induced breaking. As waves and their associated spectra undergo complex transformations during this process, several formulations have been proposed in the literature to compute an average energy dissipation rate for the wave field, which is assumed to be Rayleigh-distributed. Many of these formulations have subsequently been adapted to compute a corresponding source term for spectral modelling purposes.

DOI: 10.2112/SI95-240.1 received 31 March 2019; accepted in revision 13 February 2020.
*Corresponding author: marc.pezerat@univ-lr.fr

The main approach of these original formulations follows the work of Le Méhauté, in which the dissipation rate of a broken wave is approximated by that of a hydraulic jump of the equivalent height (often referred to as a bore model, Le Méhauté, 1962). The formulations mainly differ in the choice of the breaking criterion and the definition of the broken fraction in the original wave field.

This paper provides an extended assessment of a state-of-the-art spectral model performance under high energy conditions. Three classical depth-induced breaking formulations (Battjes and Janssen, 1978; Thornton and Guza, 1983; van der Westhuysen, 2010) are tested in the model. In particular, the role of the breaker coefficient, which is related to the bore-based energy dissipation model, is highlighted. A simple adaptive parameterization from Le Méhauté's original work (Le Méhauté, 1962) is subsequently introduced and evaluated against data collected in the shoreface of Oléron Island in the central part of the French Atlantic Coast (Figure 1a).

METHODS

This section details the data processing and presents a brief description of the modelling system with a focus on the depth-induced breaking source term.

Field Campaign and Data Processing

The field campaign was carried out by the French Hydrographic and Oceanographic Office in February 2010 to the South West of Oléron Island. This area is characterized by a very gently sloping shoreface, the isobaths 20 m being found approximately 10 km offshore (Figure 1b). During the studied period, offshore waves were characterized by a significant wave height (H_s) reaching 9 m and a mean wave period reaching 11 s (Figure 1c). These conditions correspond to a yearly return period (Lerma *et al.*, 2015) whereas yearly mean wave conditions along the 30 m

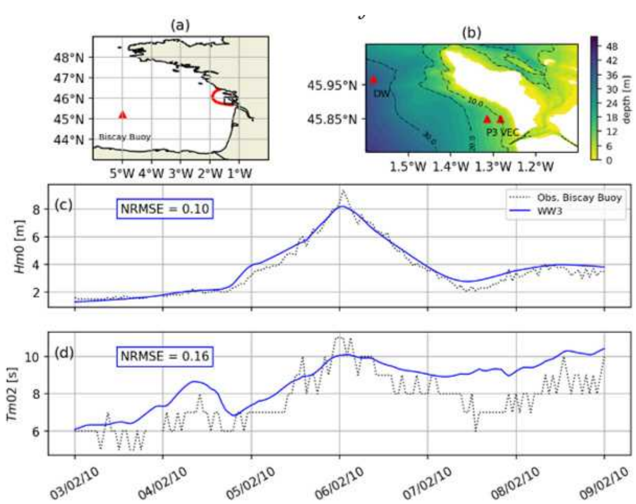

Figure 1. (a) Location of the Oléron Island in the Bay of Biscay (black box), limit of the computational domain (red dotted line) and position of the Biscay Buoy (red triangle). (b) Zoom on the study area with the bathymetry relative to MSL. Red triangles refer to the three sensors used: the DW was deployed at 33 m depth, while VEC and P3 were deployed at 13 m and 9 m depth respectively. Model/data comparison at the Biscay Buoy location: (c) H_{m0} (spectral equivalent of H_s) and (d) T_{m02} (spectral equivalent of mean period T_z).

isobaths are characterized by a significant height of 1.60 m, a mean wave period of 5.9 s and a direction of 285° from the true North (Dodet et *al.*, 2019). Data from a Datawell buoy (DW) and two pressure sensors (VEC and P3) deployed on the seabed in the nearshore area are used. For each pressure sensor, the sub-surface pressure time-series were first split into 20 minute-long bursts. Pressure measurements were corrected for sea level atmospheric pressure then, the free surface elevation signal was reconstructed using the fully dispersive nonlinear method of Bonneton and Lannes (2017), using an upper cutoff frequency set to 0.2 Hz. The elevation spectra *E(f)* were computed by means of Fast Fourier Transform using 10 Hanning-windowed segments with an overlapping of 50%. Elevation spectra were directly obtained from DW measurements. Consecutively, wave integral parameters were computed using the moments of each spectrum: $H_{m0} = 4m_0^{1/2}$; $T_{m0,2} = m_0^{1/2} m_2^{-1/2}$; $T_{pc} = m_{-2} m_1 m_0^{-2}$
where

$$m_p = \int_{fmin}^{fmax} f^p E(f)\, df \qquad (1)$$

The *fmax* value was chosen in agreement with the upper cutoff frequency used for the reconstruction of wave surface elevation from pressure sensors and a constant value of 0.04 Hz has been chosen for *fmin.*

Model Description

The third generation spectral Wind Wave Model, WWM (Roland *et al.*, 2012) is fully coupled with a circulation model within the SCHISM framework (Zhang *et al.*, 2016), where they share the same unstructured grid and domain decomposition. The wave model is forced with energy spectra obtained from a North Atlantic application of the spectral wave model WaveWatch III (WWIII; Tolman, 1991) and the tidal forcing is computed by considering the 16 main tidal constituents linearly interpolated from the regional model of Bertin *et al.* (2012). The atmospheric forcings consist of the mean sea level (MSL) pressure and 10 m wind speed taken from the Climate Forecast System Reanalysis (Saha *et al.*, 2011) for both WWM/SCHISM and WWIII models. For both wave models, the wind input and the dissipation of wave energy due to whitecapping are formulated by means of the parameterization of Ardhuin *et al*. (2010) and the non-linear quadruplet interactions are taken into account following the approach of Hasselmann and Hasselmann (1985). In shallow water, three additional processes are considered, namely the bottom friction, non-linear triad interactions and depth-induced breaking. For the first two, the JONSWAP parameterization (Hasselman *et al.*, 1973) and Eldeberky's approach (Eldeberky, 1996) are used respectively.

Depth-induced Breaking Source Term

The total energy dissipation in spectral models is distributed over frequencies and directions in proportion to the spectral energy density (Eldeberky and Battjes, 1996). The formulations for the total energy dissipation are based on the bore analogy to compute the energy dissipation rate per unit span D^* by a single breaking wave of height H in shallow water of mean depth h:

$$D^* \simeq \frac{1}{4}\rho g H^3 \sqrt{\frac{g}{h}} \simeq \frac{1}{4}\rho g (BH)^3 \sqrt{\frac{g}{h}} \qquad (2)$$

where $B = \mathcal{O}(1)$ is the breaker coefficient as presented by Thornton and Guza (1983) whereas Battjes and Janssen (1978) omited it. Le Méhauté (1962) first introduced a similar coefficient without the power 3. It accounts for the difference between the front height between of a broken wave of heigt H and that of a wave-generated bore of the same height, often referred to as a breaker and a saturated breaker. According to Le Méhauté's analytical development, the alternative equation is introduced:

$$D^* \simeq \frac{B'}{4}\rho g H^3 \sqrt{\frac{g}{h}} \; with \; B' = 40 \tan\beta \qquad (3)$$

where $\tan\beta$ is the local bottom slope.

Following the approach of Battjes and Janssen (1978) (see also Battjes and Janssen, 2009), hereafter BJ78, the overall energy dissipation is given by:

$$D = \frac{\alpha}{4} Q_b \bar{f} \rho g H_m^{\ 2} \qquad (4)$$

where α is an adjusting coefficient of order 1, Q_b corresponds to the fraction of broken waves, $\bar{f}$ is the spectral mean frequency (computed by means of $T_{m0,1}$ period) and H_m is the broken wave height. As a result, the probability density function (PDF) is clipped at H=H_m with a delta function. H_m is given by a Miche-type criterion which, in shallow water, reduces to:

$$H_m = \gamma_{BJ} h \qquad (5)$$

with $\gamma_{BJ} = 0.73$ according to Battjes and Stive (1985).

Thornton and Guza (1983), hereafter TG83, suggested that the Rayleigh distribution was still valid in the surf zone. A "distribution" of broken waves is expressed as a weighting of the PDF for all waves. As a first approach, a constant weighting function is introduced based on a depth limiting wave height criterion, following Thornton and Guza (1982) who found that the envelope for waves are depth-limited in the inner surf zone follows a linear relationship. Therefore the total dissipation is given by:

$$D = \frac{B^3}{4}\rho g \frac{f_p}{h}\int_0^{+\infty} H^3 W p(H)\, dH \qquad (6)$$

with f_p the peak frequency, $p(H)$ is the Rayleigh distribution probability density and W the weighting function given by:

$$W = \left(\frac{H_{rms}}{\gamma_{TG} h}\right)^n \qquad (7)$$

with $\gamma_{TG} = 0.42$ and $n = 4$.

Following the same approach, van der Westhuysen (2010), hereafter W10, introduced an alternative expression of the weighting function. It is based on the wave asymmetry estimated through the biphase β computed with the parameterization of Eldeberky (1996). The weighting function reads :

$$W = \left(\frac{\beta}{\beta_{ref}}\right)^n \qquad (8)$$

with $\beta_{ref} = {-4\pi}/{9}$ and $n = 2.5$. The total dissipation is given by equation (4) with f_p substituted by $\bar{f}$.

RESULTS

This section presents an extended model/data comparison based on wave integral parameters. The model error is quantified by means of the Normalized Root Mean Square Error (NRMSE) computed for each parameters.

Depth-induced Breaking Default Parameterizations

Firstly, the model's predictive skills are assessed using default parameterizations for depth-induced breaking. The coefficients α and B were set to 1, while values previously given for $\gamma_{BJ/TG}$, β_{ref} and n were unchanged compared to the original papers of BJ78, TG83 and W10. Model/data comparisons are presented in Figure 2. Water levels are well reproduced by the model, with a NRMSE of 10%. With default parameters, the three models show a severe underestimation of wave energy at the peak of the storm which worsens closer to the shore. At the DW location, in intermediate depth, $kd = \mathcal{O}(1)$, there is a maximal negative bias on H_{m0} reaching approximately 20% regardless of the breaking formulation used. It can be noticed that this bias is partially explained by a pre-existing underestimation of wave energy in the forcing spectra at the storm peak leading to a negative bias in H_{m0} reaching 12% in deep water (Figure 1c). In shallower waters, at the P3 and VEC locations, the bias on H_{m0} at peak increases and is more dependent on the depth-induced breaking formulation used. At VEC location, the negative bias on H_{m0} at peak is about 25% using BJ78 formulation, 40% using TG83 formulation and 50% using W10 formulation. This underestimation of wave energy impacts the overall statistical score on H_{m0} whereas it has little impacts on $T_{m0,2}$ and T_{pc} (see Table 1). The model results show a tidal modulation of H_{m0} at P3 location (especially for the W10 and TG83 formulations) whereas it only appears in observations at VEC location. A map of the overall energy dissipation due to depth-induced breaking using TG83 formulation is presented in Figure 3a. It demonstrates that depth-induced breaking is already substantial at P3 location whereas it is nearly absent at the DW location.

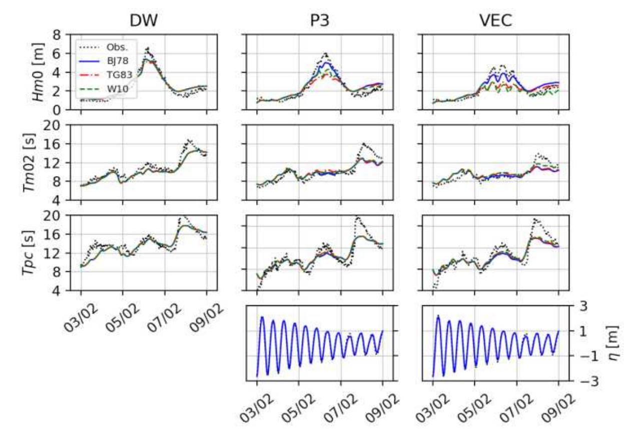

Figure 2. Model/ data comparison of water levels η, H_{m0}, $T_{m0,2}$, T_{pc} at the locations of the three sensors used: black dotted lines correspond to observations whereas model's outputs using BJ78, TG83 and W10 correspond to the blue lines, red dotted lines and green dashed lines respectively. For elevation timeseries only one model's output is being presented as the three overlap.

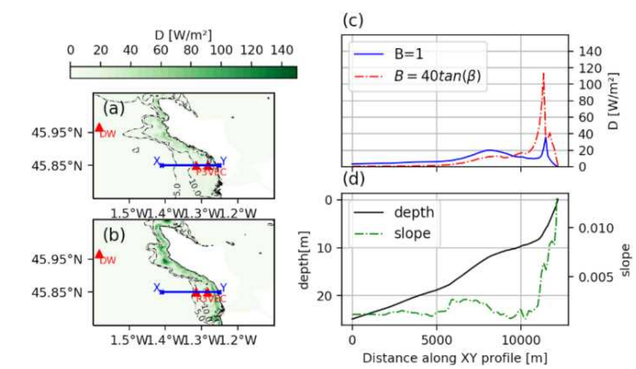

Figure 3. Maps of the energy dissipation rate associated to depth-induced breaking at the storm peak using TG83 formulation either with the default parameterization (a) or the adaptive one (b). (c) Energy dissipation rates at the storm peak along the XY profile. (d) Depth and associated slope along the XY profile.

Depth-induced Breaking Adaptive Parameterization

Subsequently, adaptive parameterization of depth-induced breaking formulations was tested with α, B^3 substituted by B' whereas the other parameters were unchanged. B' has been bound to [0,1] to be consistent with Le Méhauté's (1962). Figure 4 shows model/data comparisons. At the DW location, the same negative bias on H_{m0} is observed which is consistent with the observation made above that depth-induced breaking does not occur so far offshore (Figures 3a and 3b). At P3 and VEC locations, the bias on H_{m0} at the storm peak is considerably reduced when compared to the results with the default parameterizations. At VEC location it reduced to 15% for the BJ78 formulation and 17% for both

Table 1. *Normalized Root Mean Square Error at each location. For each breaking formulation, the first row corresponds to the default parameterization; the second row to the adaptive one.*

	DW			P3			VEC		
	H_{m0}	$T_{m0,2}$	T_{pc}	H_{m0}	$T_{m0,2}$	T_{pc}	H_{m0}	$T_{m0,2}$	T_{pc}
BJ78	0.15 0.15	0.09 0.09	0.09 0.09	0.17 0.16	0.11 0.11	0.09 0.09	0.19 0.15	0.11 0.11	0.09 0.10
TG83	0.16 0.15	0.09 0.09	0.09 0.09	0.29 0.17	0.12 0.11	0.08 0.09	0.30 0.15	0.10 0.11	0.09 0.09
W10	0.15 0.15	0.09 0.09	0.09 0.09	0.23 0.17	0.11 0.11	0.08 0.09	0.34 0.15	0.09 0.11	0.09 0.10

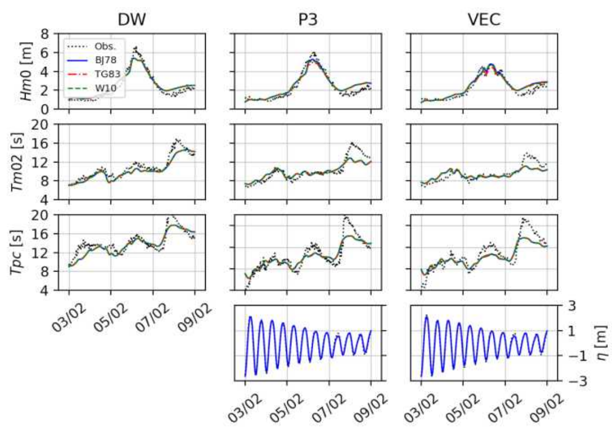

Figure 4. Same as Figure 2, but using adaptive parameterization for depth-induced breaking source terms.

TG83 and W10 formulations. The NRMSE on H_{m0} is consequently reduced to approximately 15% at each location (see Table 1). The overlapping of wave parameters time-series suggests that the model tends toward a common behaviour regardless of the formulation used for depth-induced breaking.

DISCUSSION

The default parameterizations of the three breaking formulations and the proposed breaker coefficient B' (Eq. 3) lead to very different energy dissipation rates over the Oléron shoreface at the the storm peak (Figures 3a and 3b). In the first 5 km of the extracted profile (Figures 3c and 3d), B' is less than 0.1, meaning that over this region of the shoreface, breakers are non saturated whereas default parameterizations only consider saturated breakers (*i.e.* B=1). Although the offshore dissipation rate related to default parameterization is rather small (approximately 5 W/m^2), once integrated up to the inner surf zone, it results in a substantial dissipation of waves energy and explain the underestimation of wave heights nearshore (Figure 2). Therefore, the difference of the energy dissipated by a saturated breaker and a non-saturated breaker explains the increasing over-dissipation of wave energy. This process is exacerbated by the very gently-sloping shoreface of Oléron island. The present observations do not allow to extend the comparison in the inner surf zone, where the amount of broken waves increases. Consequently, the dissipation is much more controlled by the breaking criterion which fixes the fraction of broken waves. It should be pointed out that several adaptive parameterizations of BJ78 or TG83 formulations have been proposed through *ad hoc* γ-scalings with the beach slope and/or the wave steepness (see Salmon *et al.*, 2015 for a review). More recently, Guérin *et al.* (2018) introduced a scaling in the TG83 formulation of γ_{TG} and B. These two parameters have been computed as a linear function of the bottom slope. A linear regression has been calibrated to give the best fit wave height when comparing with measurements from a field campaign. To this regard, the adaptive parameterization of the breaker coefficient introduced in this paper appears to be more robust physically (Le Méhauté, 1962) and will have to be merged with a refined parameterization of the breaking index γ. Among the possible implications of this study, the accurate modelling of storm waves has a direct impact on the computation of the wave setup, a key component of extreme water levels and related to coastal hazard (*e.g.* Guérin *et al.*, 2018). Thus, considering the 1D wave setup model of Longuet-Higgins and Stewart (1964) with a 2:1000 constant bottom slope and 6 m-high incident short waves, the adaptive parameterization for wave dissipation proposed in this study results in a wave setup two times larger compared to that obtained with a constant wave breaking parameterization. This will have to be verified in the field.

CONCLUSIONS

A state-of-the-art spectral model was used to simulate storm waves in the nearshore area. Model/data comparisons show a substantial over-dissipation of waves energy associated with depth-induced breaking for the three formulations tested with their default parameterizations. An adaptive parameterization of the breaking source terms through the breaker coefficient yields to improved predictions. This new parameterization is being tested under various incident wave conditions on case studies which include observations in the inner surf zone. Improving depth-induced breaking understanding is of primary importance for storm waves modelling which are fundamental for the nearshore dynamics.

ACKNOWLEDGMENTS

M. Pezerat is supported by a phD fellowship from CDA La Rochelle and from the FEDER project DURALIT. The study of extreme sea states is a contribution to the Chair Regional Project EVEX. K. Martins acknowledges the financial support from the University of Bordeaux, through an International Postdoctoral Grant (Idex, nb. 1024R-5030). Authors greatly acknowledge the Hydrographic and Oceanographic French Office (SHOM) for providing field observations acquired during the projects MOUTON (funded by DGA PEA 012401) and EPIGRAM (funded by LEFE/IDAO and ANR, agreement ANR-08-BLAN-033001).

LITERATURE CITED

Ardhuin, F.; Rogers, E.; Babanin, A.V.; Filipot, J.F.; Magne, R.; Roland, A.; van der Westhuysen, A.; Queffeulou, P.; Lefevre, J.M.; Aouf, L., and Collard, F., 2010. Semiempirical dissipation source functions for ocean waves. Part I: Definition, calibration, and validation. *Journal of Physical Oceanography*, 40(9), 1917-1941.

Battjes, J.A. and Janssen, J.P.F.M., 1978. Energy loss and set-up due to breaking of random waves. In *Coastal Engineering 1978*, pp. 569-587.

Battjes, J.A. and Janssen, T.T., 2009. Random wave breaking models-history and discussion. In *Coastal Engineering 2008*, 5, 25-37.

Battjes, J.A. and Stive, M.J.F., 1985. Calibration and verification of a dissipation model for random breaking waves. *Journal of Geophysical Research: Oceans*, 90(C5), 9159-9167.

Bertin, X.; Bruneau, N.; Breilh, J.F.; Fortunato, A.B., and Karpytchev, M., 2012. Importance of wave age and resonance in storm surges: The case Xynthia, Bay of Biscay. *Ocean Modelling*, 42, 16-30.

Bertin, X.; Li, K.; Roland, A., and Bidlot, J.R., 2015. The contribution of short-waves in storm surges: Two case studies in the Bay of Biscay. *Continental Shelf Research*, 96, 1-15.

Bonneton, P., and Lannes, D., 2017. Recovering water wave elevation from pressure measurements. *Journal of Fluid Mechanics*, 833, 399-429.

Dodet, G.; Bertin, X.; Bouchette, F.; Gravelle, M.; Testut, L.; and Wöppelmann, G., 2019. Characterization of sea-level variations along the metropolitan coasts of France: Waves, tides, storm surges and long-term changes. *Journal of Coastal Research* (In press).

Eldeberky, Y., 1996. Nonlinear Transformation of Wave Spectra in the Nearshore Zone. Ph.D. thesis, The Netherlands: Delft University of Technology.

Eldeberky, Y. and Battjes, J.A., 1996. Spectral modeling of wave breaking: Application to Boussinesq equations. *Journal of Geophysical Research: Oceans*, 101(C1), 1253-1264.

Guérin, T.; Bertin, X.; Coulombier, T.; and de Bakker, A., 2018. Impacts of wave-induced circulation in the surf zone on wave setup. *Ocean Modelling*, 123, 86-97.

Hasselmann, K.; Barnett, T.P.; Bouws, E.; Carlson, H., Cartwright, D.E.; Enke, K.; Ewing, J.A.; Gienapp, H.; Hasselmann, D.E. Kruseman, P.; Meerburg, A.; Müller, P.; Olbers, D.J.; Richter, K.; Sell, W., and Walden, H., 1973. Measurements of wind-wave growth and swell decay during the Joint North Sea Wave Project (JONSWAP). *Ergänzungsheft*, 8-12.

Hasselmann, S. and Hasselmann, K., 1985. Computations and parameterizations of the nonlinear energy transfer in a gravity-wave spectrum. Part I: A new method for efficient computations of the exact nonlinear transfer integral. *Journal of Physical Oceanography*, 15(11), 1369-1377.

Le Méhauté, B., 1962. On non-saturated breakers and the wave run-up. *Coastal Engineering Proceedings*, 1(8), 6.

Lerma, A.N.; Bulteau, T.; Lecacheux, S., and Idier, D., 2015. Spatial variability of extreme wave height along the Atlantic and channel French coast. *Ocean Engineering*, 97, 175-185.

Longuet-Higgins, M.S. and Stewart, R.W., 1964. Radiation stresses in water waves; a physical discussion, with applications. In *Deep Sea Research and Oceanographic Abstracts*, 11(4), 529-562.

Masselink, G.; Castelle, B.; Scott, T.; Dodet, G.; Suanez, S.; Jackson, D., and Floc'h, F., 2016. Extreme wave activity during 2013/2014 winter and morphological impacts along the Atlantic coast of Europe. *Geophysical Research Letters*, 43(5), 2135-2143.

Roland, A. and Ardhuin, F., 2014. On the developments of spectral wave models: Numerics and parameterizations for the coastal ocean. *Ocean Dynamics*, 64(6), 833-846.

Roland, A.; Zhang, Y.J.; Wang, H.V.; Meng, Y.; Teng, Y.C.; Maderich, V.; Brovchenko, I.; Dutour-Sikiric, M., and Zanke, U., 2012. A fully coupled 3D wave current interaction model on unstructured grids. *Journal of Geophysical Research: Oceans*, 117(C11).

Saha, S.; Moorthi, S.; Wu, X.; Wang, J.; Nadiga, S.; Tripp, P.; Behringer, D.; Hou, Y.T.; Chuang H.; Iredell, M.; Ek, M.; Meng, J.; Yang, R.; Mendez, M.P.; van den Dool, H.; Zhang, Q.; Wang, W.;Chen, M., and Becker, E., 2011. NCEP Climate Forecast System Version 2 (CFSv2) Selected Hourly Time-Series Products. *Research, Computational and Information Systems Laboratory*. Accessed 27 March 2019.

Salmon, J.E.; Holthuijsen, L.H.; Zijlema, M.; van Vledder, G.P., and Pietrzak, J.D., 2015. Scaling depth-induced wave-breaking in two-dimensional spectral wave models. *Ocean Modelling*, 87, 30-47.

Thornton, E.B. and Guza, R.T., 1982. Energy saturation and phase speeds measured on a natural beach. *Journal of Geophysical Research: Oceans*, 87(C12), 9499-9508.

Thornton, E.B. and Guza, R.T., 1983. Transformation of wave height distribution. *Journal of Geophysical Research: Oceans*, 88(C10), 5925-5938.

Tolman, H.L., 1991. A third-generation model for wind waves on slowly varying, unsteady, and inhomogeneous depths and currents. *Journal of Physical Oceanography*, 21(6), 782-797.

van der Westhuysen, A.J., 2010. Modeling of depth induced wave breaking under finite depth wave growth conditions. *Journal of Geophysical Research: Oceans*, 115(C1).

Zhang, Y.J., Ye, F.; Stanev, E.V., and Grashorn, S., 2016. Seamless cross-scale modeling with SCHISM. *Ocean Modelling*, 102, 64-81.